Biochemical and Biophysical Research Communications 733 (2024) 150604

Contents lists available at ScienceDirect

Biochemical and Biophysical Research Communications

journal homepage: www.elsevier.com/locate/ybbrc

# ZBTB7A forms a heterodimer with ZBTB2 and inhibits ZBTB2 homodimerization required for full activation of HIF-1

Gouki Kambe [a], Minoru Kobayashi [a,b], Hiroshi Ishikita [c,d], Sho Koyasu [a,b,e], Ester M. Hammond [f], Hiroshi Harada [a,b,*]

[a] Laboratory of Cancer Cell Biology, Graduate School of Biostudies, Kyoto University, Kyoto, Japan
[b] Department of Genome Repair Dynamics, Radiation Biology Center, Graduate School of Biostudies, Kyoto University, Kyoto, Japan
[c] Department of Applied Chemistry, The University of Tokyo, Tokyo, Japan
[d] Research Center for Advanced Science and Technology, The University of Tokyo, Tokyo, Japan
[e] Department of Diagnostic Imaging and Nuclear Medicine, Graduate School of Medicine, Kyoto University, Kyoto, Japan
[f] Department of Oncology, University of Oxford, Oxford, UK

A B S T R A C T

Hypoxia-inducible factor 1 (HIF-1), recognized as a master transcription factor for adaptation to hypoxia, is associated with malignant characteristics and therapy resistance in cancers. It has become clear that cofactors such as ZBTB2 are critical for the full activation of HIF-1; however, the mechanisms downregulating the ZBTB2-HIF-1 axis remain poorly understood. In this study, we identified ZBTB7A as a negative regulator of ZBTB2 by analyzing protein sequences and structures. We found that ZBTB7A forms a heterodimer with ZBTB2, inhibits ZBTB2 homodimerization necessary for the full expression of ZBTB2-HIF-1 downstream genes, and ultimately delays the proliferation of cancer cells under hypoxic conditions. The Cancer Genome Atlas (TCGA) analyses revealed that overall survival is better in patients with high ZBTB7A expression in their tumor tissues. These findings highlight the potential of targeting the ZBTB7A-ZBTB2 interaction as a novel therapeutic strategy to inhibit HIF-1 activity and improve treatment outcomes in hypoxia-related cancers.

## 1. Introduction

Tumor hypoxia results from an imbalance between oxygen supply and consumption in tumor tissues and is a hallmark of solid tumors. Hypoxia is strongly linked to malignant features of solid tumors, such as invasive potential, aberrant metabolism, and therapy resistance [1,2] and predicts for poor patient prognosis [3,4].

Hypoxia-inducible factor 1 (HIF-1), a heterodimeric transcription factor composed of the regulatory subunit, HIF-1α, and the constitutively expressed subunit, HIF-1β [5], is recognized as a master regulator of cellular adaptation to hypoxia [6,7]. Under normoxic conditions, HIF-1α is hydroxylated at N803 by factor inhibiting HIF-1 (FIH-1), which diminishes the interaction between HIF-1α and p300/CREB binding protein (CBP), thus suppressing HIF-1α′s transactivation activity [8]. Additionally, hydroxylation at P402 and P564 by prolyl-4-hydroxylase domain protein 1-3 (PHD1-3) triggers the ubiquitination of HIF-1α by von Hippel-Lindau protein (pVHL)-containing E3 ubiquitin ligase, leading to its proteolysis by the 26S proteasome system. Consequently, HIF-1 activity remains low under normoxic conditions. However, this negative regulation ceases under hypoxic conditions due to the inactivation of the oxygen-dependent hydroxylases [6,9–11]. Subsequently, stabilized HIF-1α, in partnership with HIF-1β, binds to hypoxia-response element (HRE) to induce the expression of various genes that contribute to tumor malignancy [12,13]. In addition to this canonical mechanism, we recently identified significant roles for upstream activators and co-activators in the full activation of HIF-1 [6,14–17], where each factor selectively enhances HIF-1 activity at different regulatory steps, influencing the expression of specific downstream genes and thus amplifying the hypoxic response. Although the mechanisms promoting HIF-1 activation are relatively well-understood, those that suppress and fine-tune its activity remain elusive.

We previously identified zinc finger and BTB-domain containing protein 2 (ZBTB2), a member of the BTB-zinc finger (BTB-ZF) family transcription factor, as a co-activator of HIF-1 [18,19]. Our findings indicate that ZBTB2 enhances HIF-1α′s transactivation activity, promoting the full expression of specific HIF-1 downstream genes and fostering the growth of p53-deficient cancers. We also discovered that homodimerization of ZBTB2, mediated by its N-terminal domain (NTD), is essential for this activity. Significantly, an NTD-mimetic polypeptide was shown to competitively inhibit ZBTB2 homodimerization and

* Corresponding author. Yoshida Konoe-cho, Sakyo-ku, Kyoto, 606-8501, Japan.
*E-mail address:* harada.hiroshi.5e@kyoto-u.ac.jp (H. Harada).

https://doi.org/10.1016/j.bbrc.2024.150604
Received 20 August 2024; Received in revised form 21 August 2024; Accepted 23 August 2024
Available online 24 August 2024

thereby suppress the ZBTB2-HIF-1 axis [19]. This observation led us to hypothesize that another BTB-ZF family protein sharing a similar amino acid sequence with the ZBTB2-NTD might also form a heterodimer with ZBTB2, thus inhibiting the ZBTB2-HIF-1 axis. In this study, we successfully identify ZBTB7A as a binding partner of ZBTB2 and demonstrate that ZBTB2-HIF-1 axis regulation is negatively affected when ZBTB2 forms a heterodimer with ZBTB7A.

## 2. Results

### 2.1. ZBTB7A interacts with ZBTB2 and inhibits ZBTB2 homodimer formation

Building on our previous discovery that a mimetic polypeptide of the ZBTB2-NTD (1–113 a.a. region) inhibits ZBTB2 homodimerization and the activity of the ZBTB2-HIF-1 axis [19], we hypothesized that a BTB-ZF family protein harboring a similar amino acid sequence with the ZBTB2-NTD might also suppress ZBTB2 activity by forming a heterodimer with ZBTB2. To identify such a negative regulator, we searched for BTB-ZF family proteins displaying high amino acid sequence identity to the ZBTB2-NTD (Fig. 1A, Table 1). Among 48 BTB-ZF proteins excluding ZBTB2 itself, ZBTB25, which has been previously reported to interact with ZBTB2 [20], showed the highest peptide sequence identity, confirming the effectiveness of this approach (Fig. 1A–Table 1). We chose to focus on ZBTB7A (also known as LRF, FBI-1, and Pokemon) since it possesses a region with 44 % identity in its N-terminus, (Fig. 1A–Table 1), and ZBTB7A has been reported to form a homodimer [21–23]. Protein sequence alignment revealed a high degree of identity between the 15–64 a.a. region of ZBTB7A and the 5–54 a.a. region of ZBTB2, which is critical for ZBTB2 homodimerization, suggesting the potential for heterodimer formation (Fig. 1B). AlphaFold 3 predictions supported that these proteins interact through salt-bridges between their helices, leading to heterodimer formation (Fig. 1C left). Moreover, the N-terminus of ZBTB7A appeared to physically mask that of ZBTB2 which is critical for ZBTB2 homodimerization (Fig. 1C right) [19]. Consequently, we investigated whether ZBTB7A physically associates with ZBTB2. HCT116 $p53^{-/-}$ cells, in which ZBTB2 homodimer was previously confirmed to upregulate HIF-1 activity [18,19], were transiently transfected with expression vectors for myc-tagged ZBTB7A and V5-tagged ZBTB2, and subjected to co-immunoprecipitation using an anti-myc tag antibody. Western blotting with an anti-V5 tag antibody confirmed that ZBTB7A forms a complex with ZBTB2 (Fig. 1D). Furthermore, to examine whether the ZBTB2-ZBTB7A heterodimerization disrupts ZBTB2 homodimerization, we performed split luciferase complementation assays that enable quantification of ZBTB2 homodimerization. ZBTB7A overexpression significantly inhibited ZBTB2 homodimerization (Fig. 1E). These findings collectively demonstrate that ZBTB7A forms a heterodimer with ZBTB2 and effectively inhibits ZBTB2 homodimerization.

### 2.2. ZBTB7A suppresses full activation of HIF-1

Next, we investigated whether the disruption of ZBTB2 homodimerization by ZBTB7A attenuates the function of ZBTB2 to enhance HIF-1 activity. We utilized a reporter system designed to quantify the transactivation (TAD) activity of HIF-1α, as we have previously established that ZBTB2 homodimerization is crucial for enhancing this activity [18,19]. Cells were transfected with two plasmids; the first expressed a fusion protein of the Gal4 DNA-binding domain (Gal4-DBD) and the HIF-1α transactivation domain (TAD: 531–826 a.a.), while the second expressed luciferase under the control of the Gal4-DBD–HIF–1α-$TAD_{531\text{-}826}$ [8,17]. We introduced P564A mutation into

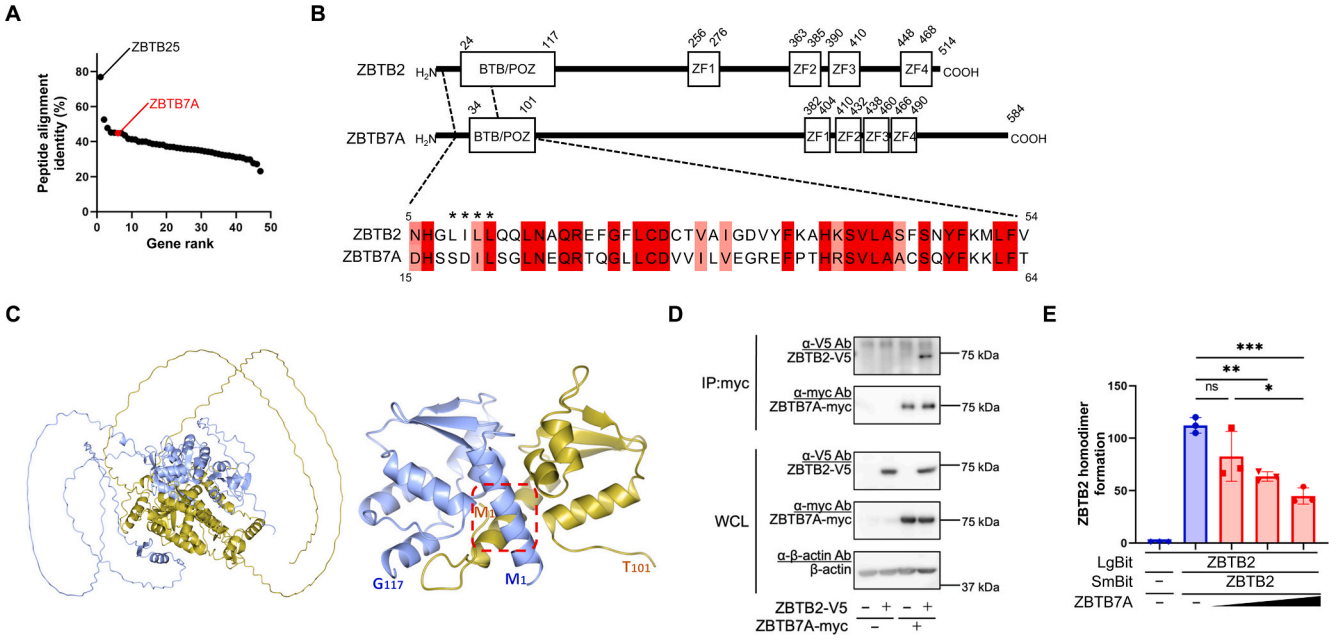


**Fig. 1. ZBTB7A interacts with ZBTB2 and inhibits ZBTB2 homodimer formation**

A) Forty-nine BTB-ZF family member proteins were subjected to the protein sequence alignment analysis with ZBTB2 NTD (1–113 a.a.) and aligned based on the identity.

B) Upper: Primary structure of ZBTB2 and ZBTB7A. Lower: Peptide sequence alignment analysis of the ZBTB2 NTD (5–54 a.a.) and ZBTB7A NTD (15–64 a.a.). Asterisks show crucial amino acids for ZBTB2 homodimerization.

C) Predicted structures of heterodimer composed of full-length (left) or N-terminal regions (right) of ZBTB2 (cyan) and ZBTB7A (yellow).

D) Upper: co-IP using anti-myc tag antibody followed by Western blotting using the indicated antibodies for HCT116 $p53^{-/-}$ cells transfected with plasmids expressing ZBTB2-V5, ZBTB7A-myc or corresponding empty vector (−). Lower: Western blotting for whole-cell-lysate (WCL).

E) Split luciferase complementation assay to quantify ZBTB2 homodimerization in HCT116 $p53^{-/-}$ cells transfected with the indicated combination of plasmids expressing ZBTB2-LgBit, either ZBTB2-SmBit or its empty vector (−), and either ZBTB7A or its empty vector (−) at three concentrations. Mean ± s.d. One-way ANOVA with Turkey's test. ns: not significant, $*p < 0.05$, $**p < 0.01$, $***p < 0.001$.

**Table 1**
Protein sequence identity between 49 BTB-ZF proteins and ZBTB2-NTD (1–113 a.a. region).

| rank | BTB-ZF proteins | identity to ZBTB2-NTD (%) |
|---|---|---|
| 1 | ZBTB25 | 76.9 |
| 2 | ZBTB49 | 52.6 |
| 3 | ZBTB4 | 47.8 |
| 4 | MIZ1 (ZBTB17) | 45.3 |
| 5 | ZNF913 (ZBTB11) | 45.1 |
| 6 | ZBTB7a | 44.9 |
| 7 | ZBTB7b | 44.9 |
| 8 | ZBTB1 | 43.6 |
| 9 | ZBTB48 | 41.7 |
| 10 | HIC2 (ZBTB30) | 41.4 |
| 11 | ZBTB40 | 41.2 |
| 12 | HIC1 (ZBTB29) | 40.0 |
| 13 | PATZ1 (ZBTB19) | 40.0 |
| 14 | ZBTB44 | 40.0 |
| 15 | ZBTB5 | 39.3 |
| 16 | CIBZ (ZBTB38) | 38.8 |
| 17 | ZFP161 (ZBTB14) | 38.6 |
| 18 | ZNF295 (ZBTB21) | 38.3 |
| 19 | ZBTB8a | 38.2 |
| 20 | ZFP238 (ZBTB18) | 37.2 |
| 21 | ZBTB10 | 37.0 |
| 22 | ZBTB43 | 36.9 |
| 23 | ZBTB3 | 36.5 |
| 24 | MYNN (ZBTB31) | 36.3 |
| 25 | ZBTB39 | 36.0 |
| 26 | ZBTB42 | 35.7 |
| 27 | ZBTB26 | 35.6 |
| 28 | KAISO (ZBTB33) | 35.4 |
| 29 | ZBTB9 | 35.2 |
| 30 | ZBTB7c | 34.9 |
| 31 | ZBTB22 | 34.5 |
| 32 | ZBTB34 | 34.2 |
| 33 | ZBTB46 | 33.9 |
| 34 | ZBTB45 | 33.3 |
| 35 | ZBTB8b | 33.0 |
| 36 | GZF1 (ZBTB23) | 32.5 |
| 37 | ZFP131 (ZBTB35) | 32.2 |
| 38 | ZBTB37 | 32.0 |
| 39 | ZBTB16 | 31.7 |
| 40 | ZBTB41 | 31.2 |
| 41 | PATZ2 (ZBTB24) | 31.1 |
| 42 | BCL6 (ZBTB27) | 30.7 |
| 43 | ZFP651 (ZBTB47) | 29.9 |
| 44 | ZBTB6 | 29.8 |
| 45 | ZBTB32 | 27.7 |
| 46 | ZBTB20 | 27.2 |
| 47 | ZBTB12 | 23.2 |
| 48 | BCL6B (ZBTB28) | not detected |

the HIF-1α $TAD_{531\text{-}826}$ of the first plasmid to eliminate the influence of oxygen-dependent degradation of Gal4-DBD–HIF–1α $TAD_{531\text{-}826}$ [17]. The HIF-1α TAD assay revealed that ZBTB7A overexpression suppressed the ZBTB2-mediated activation of HIF-1α TAD activity without negatively impacting on the expression levels of ZBTB2 and the Gal4-DBD–HIF–1α TAD proteins (Fig. 2A and B).

We also assessed the effect of ZBTB7A on ZBTB2 activity using another reporter assay system. Previously, we identified Stanniocalcin 1 (STC1) as a downstream gene induced by the ZBTB2-HIF-1 axis at the transcription initiation levels [19,24]; therefore, we constructed a reporter plasmid linking the STC1 promoter to luciferase. Consequently, the reporter showed that STC1 promoter activity, which increased under hypoxic conditions, was further enhanced by ZBTB2 (Fig. 2C). This enhancement was completely negated by the ZBTB7A expression without reducing the protein levels of ZBTB2 and HIF-1α (Fig. 2C and D).

Subsequently, we investigated whether ZBTB7A downregulates the expression of endogenous ZBTB2-HIF-1 downstream genes. qRT-PCR for representative downstream genes, STC1 and paired box 8 (PAX8), verified that their expression was elevated upon hypoxia and further enhanced by ZBTB2 in the absence of ZBTB7A overexpression (Fig. 2E and F). This enhancement was significantly reduced by ZBTB7A in the presence of HIF-1α under hypoxic conditions, confirming the inhibitory role of ZBTB7A.

Together, these results demonstrate that the physical interaction between ZBTB7A and ZBTB2 inhibits ZBTB2 homodimerization, subsequently preventing ZBTB2-mediated full activation of HIF-1 and thus reducing the expression of ZBTB2-HIF-1 downstream genes.

### *2.3. ZBTB7A suppresses cancer cell proliferation by disrupting ZBTB2 homodimer under hypoxia, and low ZBTB7A expression is associated with poor prognosis in renal cancer patients*

As aberrant expression of STC1 and PAX8 is linked to cancer cell proliferation [25,26], we analyzed whether ZBTB7A could delay cancer cell proliferation by inhibiting ZBTB2 homodimerization. As previously reported, a colorimetric cell proliferation assay confirmed that the ZBTB2 N-terminus-mimetic polypeptide, ZBTB2[1–113], which was reported to inhibit ZBTB2 homodimerization [19], significantly delayed cancer cell proliferation in the presence of HIF-1α under hypoxic conditions (Fig. 3A and B). ZBTB7A also delayed proliferation to the same extent as ZBTB2[1–113] (Fig. 3A and B). Importantly, the effect achieved by simultaneous introduction of ZBTB7A and ZBTB2[1–113] was equivalent to that by either of them alone (Fig. 3A and B), indicating that ZBTB7A suppresses cancer cell proliferation through the same mechanism as ZBTB2[1–113] by inhibiting ZBTB2 homodimerization.

Finally, we examined the relationship between intratumoral ZBTB7A expression levels and the prognosis in cancer patients. We focused on renal cancer patients because HIF-α is known to be stabilized due to mutations in VHL and TCEB1 [27,28]. Kaplan-Meier analysis using TCGA database demonstrated that renal cancer patients with low ZBTB7A expression exhibited significantly poorer overall survival compared to those with high ZBTB7A expression (Fig. 3C).

## 3. Discussion

In this study, we unveiled a novel regulatory mechanism whereby ZBTB7A, a member of the BTB-ZF family, acts as a negative regulator of ZBTB2 by forming a heterodimer that disrupts ZBTB2 homodimer formation. This interaction crucially suppresses full activation of HIF-1 mediated by the ZBTB2 homodimer, consequently reducing the expression of downstream target genes and the proliferation of cancer cells under hypoxic conditions. Importantly, we also observed that lower intratumoral expression levels of ZBTB7A correlate with poorer prognosis in renal cancer patients, suggesting that ZBTB7A may play a protective role in tumor progression by modulating ZBTB2 activity.

The inhibition of ZBTB2 homodimerization by ZBTB7A highlights a potential therapeutic strategy for manipulating HIF-1 activity in tumors. The clinical correlation between low ZBTB7A expression and poorer outcomes further emphasizes its importance. Several reports have consistently suggested the function of ZBTB7A as a tumor suppressor in various types of cancer [29–32]. However, ZBTB7A was initially reported as an oncogene in lymphomas due to its activity in repressing the ARF-MDM2-p53 pathway [33], and accumulating evidence also indicates ZBTB7A overexpression in some cancer types [21,29]. Thus, since the role of ZBTB7A in tumorigenesis seems complex and context-dependent, further investigation is required to develop strategies to inhibit HIF activity by modulating ZBTB7A.

A limitation of this study is the lack of a broader genome-wide analysis of other BTB-ZF family members, which may also regulate ZBTB2 activity because previous studies have suggested the interaction of ZBTB2 with ZBTB25, ZBTB28, ZBTB42, and ZBTB49 [19,20,34]. Moreover, how ZBTB7A expression is regulated and its impact on ZBTB2 activity remain unclear. Additionally, although we have reported that the effect of ZBTB2 on HIF-1 is observed only in p53-deficient cells, whether ZBTB7A is involved in the p53-dependence remains to be

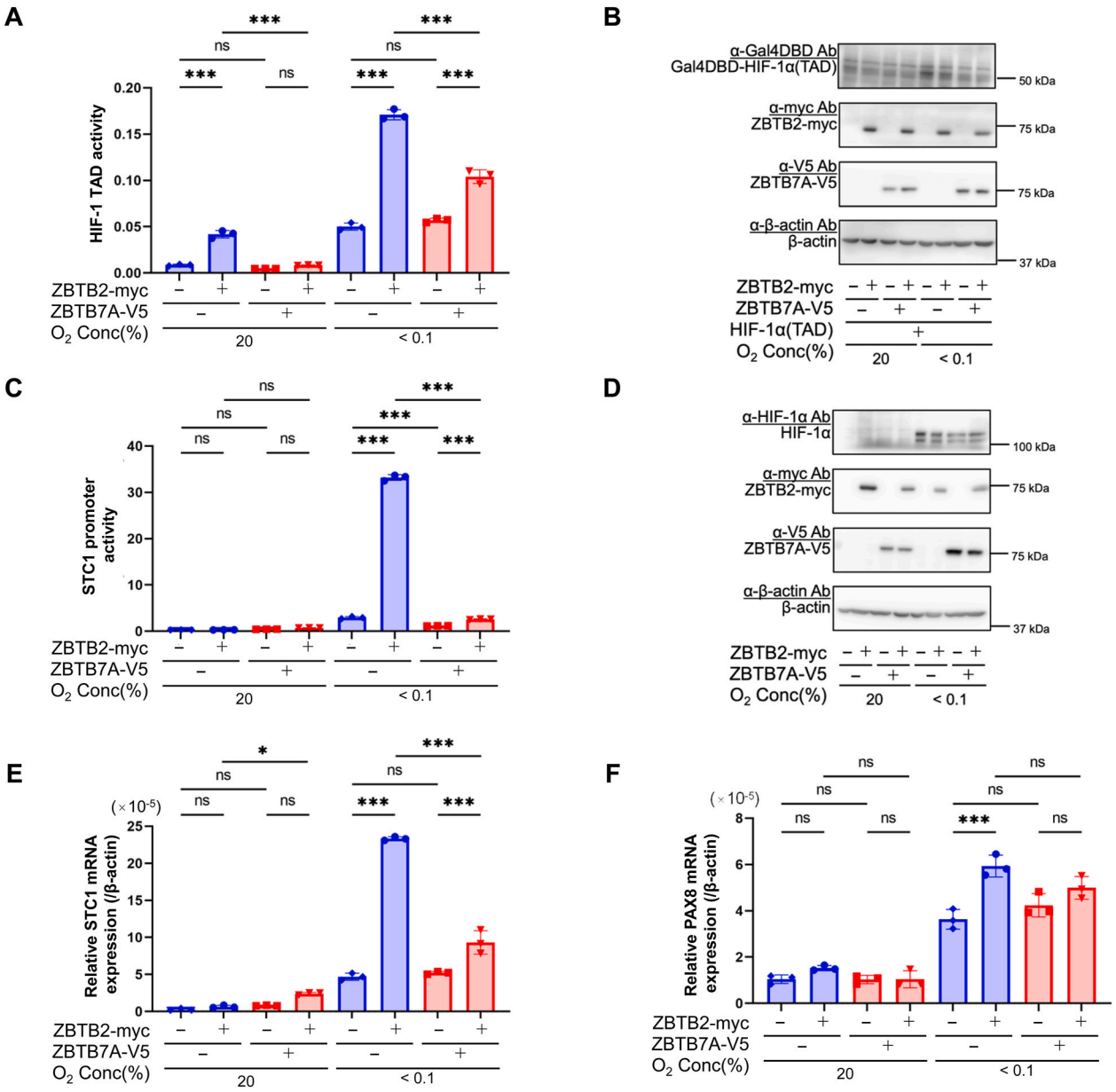


**Fig. 2. ZBTB7A suppresses full activation of HIF-1**

A-F) Luciferase assay for HIF-1α TAD activity (A), luciferase assay for STC1 promoter activity (C), and qRT-PCR for STC1 (E) and PAX8 (F) mRNAs in HCT116 $p53^{-/-}$ cells transiently transfected with the plasmids expressing the indicated proteins or its corresponding empty vector (−) and cultured under the indicated oxygen conditions. Western blotting using the cell lysates harvested in A (B) and C (D) for the indicated proteins.

Means ± s.d. (A,C,E,F). One-way ANOVA with Turkey's test. ns: not significant, *$p < 0.05$, ***$p < 0.001$.

elucidated. Addressing these questions could open new avenues for the development of targeted therapies that improve patient outcomes by suppressing hypoxia-driven cancer progression.

## 4. Material & methods

### 4.1. Cell culture

A cervical cancer cell line, HeLa, purchased from the American Type Culture Collection and HCT116 $p53^{-/-}$ cells, a generous gift from Prof. Bert Vogelstein, were cultured in DMEM (Nacalai) with 10 % heat-inactivated fetal bovine serum (EQUITECH-BIO) and 1 % penicillin-streptomycin (Nacalai) at 37 °C in a well-humidified incubator with 5 % $CO_2$. For hypoxic treatments, cells were cultured in a well-humidified atmosphere of 5 % $CO_2$ and <0.1 % $O_2$ using INVIVO2 500 Hypoxic Work Station (Ruskinn Technology Limited).

### 4.2. Plasmid constructs and transient transfection

pEF6/ZBTB2 [1–113] was constructed previously [19]. To construct pEF6B/ZBTB7A-myc and pcDNA6B/ZBTB7A-V5, the DNA fragment encoding ZBTB7A was amplified from HCT116 $p53^{-/-}$ cDNA by PCR using the primers, 5′-tatgaattcgccaccatggccggcggcgtggacgg-3′ and 5′-tattctagactggcgagtccggctgtgaagttacc-3′, digested with *Eco*RI and *Xba*I, and inserted into the corresponding sites of pEF6/myc-His B and pcDNA6/V5-His B (Invitrogen), respectively. To construct

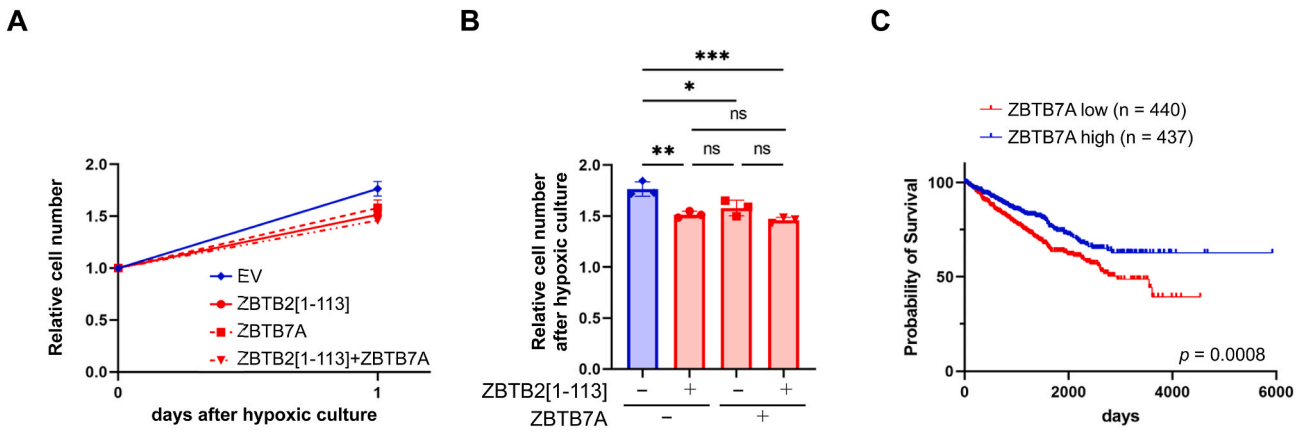


**Fig. 3. ZBTB7A suppresses cancer cell proliferation by disrupting ZBTB2 homodimer under hypoxia, and low ZBTB7A expression is associated with poor prognosis in renal cancer patients**

A,B) Colorimetric cell proliferation assay using cells transiently transfected with plasmids expressing the indicated protein or its empty vector (EV) before (day 0) and 1-day after (day 1) hypoxic (1 % $O_2$) treatment. Data on day-1 is extracted from A (B). Means ± s.d. One-way ANOVA with Turkey's test. ns: not significant, $*p < 0.05$, $**p < 0.01$ $***p < 0.001$.

C) TCGA-based Kaplan–Meier analysis of overall survival of renal cancer patients stratified by ZBTB7A expression levels; low (red: n = 440) and high (blue: n = 437), Log-rank test, $p = 0.0008$.

pGL4.23/STC1p-luc, the DNA fragment of STC1 locus (from +560 to +1645) containing HRE was amplified from HCT116 $p53^{-/-}$ genomic DNA by PCR using primers, 5′-aatagccttaggcagtggagc-3′ and 5′-agactggaagaaaaccgcaa-3′, digested with *Sac*I and *Bgl*II, and inserted into the corresponding site of pGL4.23[minP/luc2] (Promega). Transient transfections were performed using PEI MAX (Polysciences), according to the manufacturer's instructions.

### 4.3. Structural analysis

AlphaFold 3 [35] was used to predict the structures of the ZBTB2-ZBTB7A heterodimer based on their amino acid sequences. Five potential structures were generated, and the highest-ranked structure was selected for further analysis. The atomic coordinates are provided in the Supporting Information.

### 4.4. Co-immunoprecipitation (co-IP)

HCT116 $p53^{-/-}$ cells were cultured overnight, transfected with the indicated plasmids, and cultured for an additional 48 h. Cell lysates were harvested in cell lysis buffer (20 mM Tris-HCl pH = 7.5, 250 mM NaCl, 0.5 % NP-40) containing 1 × ProteoGuard™ EDTA-Free Protease Inhibitor Cocktail (Takara) and 50 μM MG132 (Merck). The lysates were sonicated with Bioruptor UCW-210 (Cosmo Bio) and one-tenth of the supernatant collected by centrifugation was subjected to Western blotting as WCL samples, and remaining nine-tenths were subjected to co-IP using anti-myc tag antibody (Cell Signaling Technology), as described previously [19].

### 4.5. Western blotting

Target proteins were detected by incubating the membranes overnight at 4 °C with primary antibodies against β-actin (Santa Cruz), myc tag (Cell Signaling Technology), HIF-1α (BD Biosciences), V5 tag (MBL) and Gal4DBD (Santa Cruz), all diluted 1:500 in Solution I (Toyobo). Signals were detected with mouse IgG HRP-linked secondary antibody (Cytiva) and ECL Prime Western Blotting Detection Reagents (Cytiva), as described previously [19].

### 4.6. Quantitative real-time PCR (qRT-PCR)

HCT116 $p53^{-/-}$ cells were cultured overnight, and transfected with indicated plasmids. Twenty-four hours later, cells were additionally cultured under hypoxic conditions for 24 h and subjected to qRT-PCR using forward primer: 5′-TGGCACCCAGCACAATGAA-3′ and reverse primer: 5′-CTAAGTCATAGTCCGCCTAGAAGC-3′ for human ACTB, using forward primer: 5′-AAGCCATCACTGAGGTCGTC-3′ and reverse primer: 5′-CAGGCTTCGGACAAGTCTGT-3′ for human STC1, and using forward primer: 5′-CATTTGAGCGGCAGCACTAC-3′ and reverse primer: 5′-AAGGGTGAGTGAGGATCTGC-3′ for human PAX8, as described previously [19].

### 4.7. Split luciferase complementation assay

HCT116 $p53^{-/-}$ cells transiently transfected with the plasmids expressing ZBTB2-LgBit and either ZBTB2-SmBit or its empty vector [19] were re-seeded into 96-well plates, cultured under normoxic or hypoxic condition for 24 h, and subjected to luciferase assay using Nano-Glo Live Cell Assay System (Promega), according to the manufacturer's instructions.

### 4.8. Luciferase assay

HCT116 $p53^{-/-}$ cells were cultured overnight and transfected with the combination of pG5E1bLuc, pcDNA6/Gal4 DBD–HIF–1α $TAD_{531\text{-}826}$ P564A, and pRL-TK (Promega) or with pGL4.23/STC1p-luc and pRL-TK. Twenty-four hours later, the cells were cultured under normoxic or hypoxic condition for another 24 h and subjected to Dual-Luciferase Reporter Assay (Promega), according to the manufacturer's instructions.

### 4.9. Colorimetric cell proliferation assay

HeLa cells transiently transfected with the combination of either pEF6/ZBTB2 [1–113] or its empty vector (pEF6/myc-His B) and either pcDNA6B/ZBTB7A-V5 or its empty vector (pcDNA6/V5-His B) were re-seeded into 96-well plates and cultured for 24 h. Then, just before and 24 h after hypoxic treatment (1 % $O_2$ using INVIVO2 400 Hypoxic Work Station), the number of cells were quantified using Cell Count Reagent SF (Nacalai tesque), according to the manufacturer's instructions.

### 4.10. TCGA analysis

TCGA RNA seq datasets were obtained from GDC Data Portal (https://portal.gdc.cancer.gov) *via* Human Protein Atlas (https://www.

proteinatlas.org/). Renal cancer patient samples were classified whether ZBTB7A expression levels exceeded the median level and overall survival was analyzed by the Kaplan–Meier method and compared by log-rank test.

### 4.11. Quantification and statistical analysis

Data represent means from at least 3 independent experiments. Statistical significance was assessed using one-way ANOVA followed by Turkey's tests, with $p < 0.05$ considered statistically significant.

## CRediT authorship contribution statement

**Gouki Kambe:** Writing – original draft, Investigation, Funding acquisition, Formal analysis, Conceptualization. **Minoru Kobayashi:** Writing – review & editing, Formal analysis, Conceptualization. **Hiroshi Ishikita:** Writing – review & editing, Investigation, Funding acquisition, Formal analysis. **Sho Koyasu:** Writing – review & editing, Resources. **Ester M. Hammond:** Writing – review & editing, Formal analysis. **Hiroshi Harada:** Writing – review & editing, Writing – original draft, Funding acquisition, Formal analysis, Conceptualization.

## Declaration of competing interest

The authors declare no competing interests.

## Acknowledgements

This study was supported by the AMED-CREST (24gm1110010s0306) and the Promotion of Cancer Research and Therapeutic Evolution (P-PROMOTE: 24ama221417h0003) to H.H. from the Japan Agency for Medical Research and development (AMED), by the Core-to-Core Program (JPJSCCA20200009) to H.H. and KAKENHI (23H02855, 23K27546, and 23K18274 to H.H. and JP23H02444 to H.I.) from the Japan Society for the Promotion of Science (JSPS), by the research grant programs of the Princess Takamatsu Cancer Research Fund, Takeda Science Foundation, Ichiro Kanehara Foundation for the Promotion of Medical Sciences and Medical Care, Kobayashi Foundation for Cancer Research, and the Foundation for Promotion of Cancer Research to H.H., by Kyoto University Division of Graduate Studies SPRING Program to G.K., and by Interdisciplinary Computational Science Program in CCS, University of Tsukuba to H.I.

## Appendix A. Supplementary data

Supplementary data to this article can be found online at https://doi.org/10.1016/j.bbrc.2024.150604.

## References

[1] P. Vaupel, L. Harrison, Tumor hypoxia: causative factors, compensatory mechanisms, and cellular response, Oncol. 9 (Suppl 5) (2004) 4–9, https://doi.org/10.1634/theoncologist.9-90005-4.
[2] P. Vaupel, K. Schlenger, C. Knoop, M. Hockel, Oxygenation of human tumors: evaluation of tissue oxygen distribution in breast cancers by computerized O2 tension measurements, Cancer Res. 51 (1991) 3316–3322.
[3] B.W. Miller, J.P. Morton, M. Pinese, G. Saturno, N.B. Jamieson, E. McGhee, P. Timpson, J. Leach, L. McGarry, E. Shanks, P. Bailey, D. Chang, K. Oien, S. Karim, A. Au, C. Steele, C.R. Carter, C. McKay, K. Anderson, T.R. Evans, R. Marais, C. Springer, A. Biankin, J.T. Erler, O.J. Sansom, Targeting the LOX/hypoxia axis reverses many of the features that make pancreatic cancer deadly: inhibition of LOX abrogates metastasis and enhances drug efficacy, EMBO Mol. Med. 7 (2015) 1063–1076, https://doi.org/10.15252/emmm.201404827.
[4] P. Vaupel, Hypoxia and aggressive tumor phenotype: implications for therapy and prognosis, Oncol. 13 (Suppl 3) (2008) 21–26, https://doi.org/10.1634/theoncologist.13-S3-21.
[5] G.L. Wang, B.H. Jiang, E.A. Rue, G.L. Semenza, Hypoxia-inducible factor 1 is a basic-helix-loop-helix-PAS heterodimer regulated by cellular O2 tension, Proc. Natl. Acad. Sci. U. S. A. 92 (1995) 5510–5514, https://doi.org/10.1073/pnas.92.12.5510.
[6] S. Koyasu, M. Kobayashi, Y. Goto, M. Hiraoka, H. Harada, Regulatory mechanisms of hypoxia-inducible factor 1 activity: two decades of knowledge, Cancer Sci. 109 (2018) 560–571, https://doi.org/10.1111/cas.13483.
[7] G.L. Semenza, Targeting HIF-1 for cancer therapy, Nat. Rev. Cancer 3 (2003) 721–732, https://doi.org/10.1038/nrc1187.
[8] P.C. Mahon, K. Hirota, G.L. Semenza, FIH-1: a novel protein that interacts with HIF-1alpha and VHL to mediate repression of HIF-1 transcriptional activity, Genes Dev. 15 (2001) 2675–2686, https://doi.org/10.1101/gad.924501.
[9] M. Ohh, C.W. Park, M. Ivan, M.A. Hoffman, T.Y. Kim, L.E. Huang, N. Pavletich, V. Chau, W.G. Kaelin, Ubiquitination of hypoxia-inducible factor requires direct binding to the beta-domain of the von Hippel-Lindau protein, Nat. Cell Biol. 2 (2000) 423–427, https://doi.org/10.1038/35017054.
[10] P.H. Maxwell, M.S. Wiesener, G.W. Chang, S.C. Clifford, E.C. Vaux, M.E. Cockman, C.C. Wykoff, C.W. Pugh, E.R. Maher, P.J. Ratcliffe, The tumour suppressor protein VHL targets hypoxia-inducible factors for oxygen-dependent proteolysis, Nature 399 (1999) 271–275, https://doi.org/10.1038/20459.
[11] S. Salceda, J. Caro, Hypoxia-inducible factor 1alpha (HIF-1alpha) protein is rapidly degraded by the ubiquitin-proteasome system under normoxic conditions. Its stabilization by hypoxia depends on redox-induced changes, J. Biol. Chem. 272 (1997) 22642–22647, https://doi.org/10.1074/jbc.272.36.22642.
[12] E.E. Wicks, G.L. Semenza, Hypoxia-inducible factors: cancer progression and clinical translation, J. Clin. Invest. 132 (2022), https://doi.org/10.1172/JCI159839.
[13] A. Nagao, M. Kobayashi, S. Koyasu, C.C.T. Chow, H. Harada, HIF-1-Dependent reprogramming of glucose metabolic pathway of cancer cells and its therapeutic significance, Int. J. Mol. Sci. 20 (2019), https://doi.org/10.3390/ijms20020238.
[14] M. Kobayashi, A. Morinibu, S. Koyasu, Y. Goto, M. Hiraoka, H. Harada, A circadian clock gene, PER2, activates HIF-1 as an effector molecule for recruitment of HIF-1alpha to promoter regions of its downstream genes, FEBS J. 284 (2017) 3804–3816, https://doi.org/10.1111/febs.14280.
[15] C.J. Yeom, L. Zeng, Y. Goto, A. Morinibu, Y. Zhu, K. Shinomiya, M. Kobayashi, S. Itasaka, M. Yoshimura, C.G. Hur, H. Kakeya, E.M. Hammond, M. Hiraoka, H. Harada, LY6E: a conductor of malignant tumor growth through modulation of the PTEN/PI3K/Akt/HIF-1 axis, Oncotarget 7 (2016) 65837–65848, https://doi.org/10.18632/oncotarget.11670.
[16] Y. Goto, L. Zeng, C.J. Yeom, Y. Zhu, A. Morinibu, K. Shinomiya, M. Kobayashi, K. Hirota, S. Itasaka, M. Yoshimura, K. Tanimoto, M. Torii, T. Sowa, T. Menju, M. Sonobe, H. Kakeya, M. Toi, H. Date, E.M. Hammond, M. Hiraoka, H. Harada, UCHL1 provides diagnostic and antimetastatic strategies due to its deubiquitinating effect on HIF-1alpha, Nat. Commun. 6 (2015) 6153, https://doi.org/10.1038/ncomms7153.
[17] L. Zeng, A. Morinibu, M. Kobayashi, Y. Zhu, X. Wang, Y. Goto, C.J. Yeom, T. Zhao, K. Hirota, K. Shinomiya, S. Itasaka, M. Yoshimura, G. Guo, E.M. Hammond, M. Hiraoka, H. Harada, Aberrant IDH3alpha expression promotes malignant tumor growth by inducing HIF-1-mediated metabolic reprogramming and angiogenesis, Oncogene 34 (2015) 4758–4766, https://doi.org/10.1038/onc.2014.411.
[18] C.C.T. Chow, M. Kobayashi, G. Kambe, H. Harada, ZBTB2 is recruited to a specific subset of HIF-1 target loci to facilitate full gene expression under hypoxia, J. Mol. Biol. 435 (2023) 168162, https://doi.org/10.1016/j.jmb.2023.168162.
[19] S. Koyasu, S. Horita, K. Saito, M. Kobayashi, H. Ishikita, C.C. Chow, G. Kambe, S. Nishikawa, T. Menju, A. Morinibu, Y. Okochi, Y. Tabuchi, Y. Onodera, N. Takeda, H. Date, G.L. Semenza, E.M. Hammond, H. Harada, ZBTB2 links p53 deficiency to HIF-1-mediated hypoxia signaling to promote cancer aggressiveness, EMBO Rep. 24 (2023) e54042, https://doi.org/10.15252/embr.202154042.
[20] I.D. Karemaker, M. Vermeulen, ZBTB2 reads unmethylated CpG island promoters and regulates embryonic stem cell differentiation, EMBO Rep. 19 (2018), https://doi.org/10.15252/embr.201744993.
[21] S. Gupta, A.K. Singh, K.S. Prajapati, P.P. Kushwaha, M. Shuaib, S. Kumar, Emerging role of ZBTB7A as an oncogenic driver and transcriptional repressor, Cancer Lett. 483 (2020) 22–34, https://doi.org/10.1016/j.canlet.2020.04.015.
[22] O.M. Siggs, B. Beutler, The BTB-ZF transcription factors, Cell Cycle 11 (2012) 3358–3369, https://doi.org/10.4161/cc.21277.
[23] N. Sakurai, M. Maeda, S.U. Lee, Y. Ishikawa, M. Li, J.C. Williams, L. Wang, L. Su, M. Suzuki, T.I. Saito, S. Chiba, S. Casola, H. Yagita, J. Teruya-Feldstein, S. Tsuzuki, R. Bhatia, T. Maeda, The LRF transcription factor regulates mature B cell development and the germinal center response in mice, J. Clin. Invest. 121 (2011) 2583–2598, https://doi.org/10.1172/JCI45682.
[24] H.Y. Yeung, K.P. Lai, H.Y. Chan, N.K. Mak, G.F. Wagner, C.K. Wong, Hypoxia-inducible factor-1-mediated activation of stanniocalcin-1 in human cancer cells, Endocrinology 146 (2005) 4951–4960, https://doi.org/10.1210/en.2005-0365.
[25] R.R. Kakun, Z. Melamed, R. Perets, PAX8 in the junction between development and tumorigenesis, Int. J. Mol. Sci. 23 (2022), https://doi.org/10.3390/ijms23137410.
[26] F. Zhao, G. Yang, M. Feng, Z. Cao, Y. Liu, J. Qiu, L. You, L. Zheng, T. Zhang, Y. Zhao, Expression, function and clinical application of stanniocalcin-1 in cancer, J. Cell Mol. Med. 24 (2020) 7686–7696, https://doi.org/10.1111/jcmm.15348.
[27] Y. Sato, T. Yoshizato, Y. Shiraishi, S. Maekawa, Y. Okuno, T. Kamura, T. Shimamura, A. Sato-Otsubo, G. Nagae, H. Suzuki, Y. Nagata, K. Yoshida, A. Kon, Y. Suzuki, K. Chiba, H. Tanaka, A. Niida, A. Fujimoto, T. Tsunoda, T. Morikawa, D. Maeda, H. Kume, S. Sugano, M. Fukayama, H. Aburatani, M. Sanada, S. Miyano, Y. Homma, S. Ogawa, Integrated molecular analysis of clear-cell renal cell carcinoma, Nat. Genet. 45 (2013) 860–867, https://doi.org/10.1038/ng.2699.
[28] W.G. Kaelin Jr., The von Hippel-Lindau tumour suppressor protein: O2 sensing and cancer, Nat. Rev. Cancer 8 (2008) 865–873, https://doi.org/10.1038/nrc2502.
[29] C. Constantinou, M. Spella, V. Chondrou, G.P. Patrinos, A. Papachatzopoulou, A. Sgourou, The multi-faceted functioning portrait of LRF/ZBTB7A, Hum. Genom. 13 (2019) 66, https://doi.org/10.1186/s40246-019-0252-0.

[30] L. Hartmann, S. Dutta, S. Opatz, S. Vosberg, K. Reiter, G. Leubolt, K.H. Metzeler, T. Herold, S.A. Bamopoulos, K. Braundl, E. Zellmeier, B. Ksienzyk, N.P. Konstandin, S. Schneider, K.P. Hopfner, A. Graf, S. Krebs, H. Blum, J.M. Middeke, F. Stolzel, C. Thiede, S. Wolf, S.K. Bohlander, C. Preiss, L. Chen-Wichmann, C. Wichmann, M. C. Sauerland, T. Buchner, W.E. Berdel, B.J. Wormann, J. Braess, W. Hiddemann, K. Spiekermann, P.A. Greif, ZBTB7A mutations in acute myeloid leukaemia with t (8;21) translocation, Nat. Commun. 7 (2016) 11733, https://doi.org/10.1038/ncomms11733.

[31] J. Guarnerio, L. Riccardi, R. Taulli, T. Maeda, G. Wang, R.M. Hobbs, M.S. Song, P. Sportoletti, R. Bernardi, R.T. Bronson, M. Castillo-Martin, C. Cordon-Cardo, A. Lunardi, P.P. Pandolfi, A genetic platform to model sarcomagenesis from primary adult mesenchymal stem cells, Cancer Discov. 5 (2015) 396–409, https://doi.org/10.1158/2159-8290.CD-14-1022.

[32] G. Wang, A. Lunardi, J. Zhang, Z. Chen, U. Ala, K.A. Webster, Y. Tay, E. Gonzalez-Billalabeitia, A. Egia, D.R. Shaffer, B. Carver, X.S. Liu, R. Taulli, W.P. Kuo, C. Nardella, S. Signoretti, C. Cordon-Cardo, W.L. Gerald, P.P. Pandolfi, Zbtb7a suppresses prostate cancer through repression of a Sox9-dependent pathway for cellular senescence bypass and tumor invasion, Nat. Genet. 45 (2013) 739–746, https://doi.org/10.1038/ng.2654.

[33] T. Maeda, R.M. Hobbs, T. Merghoub, I. Guernah, A. Zelent, C. Cordon-Cardo, J. Teruya-Feldstein, P.P. Pandolfi, Role of the proto-oncogene Pokemon in cellular transformation and ARF repression, Nature 433 (2005) 278–285, https://doi.org/10.1038/nature03203.

[34] D. Olivieri, S. Paramanathan, A.F. Bardet, D. Hess, S.A. Smallwood, U. Elling, J. Betschinger, The BTB-domain transcription factor ZBTB2 recruits chromatin remodelers and a histone chaperone during the exit from pluripotency, J. Biol. Chem. 297 (2021) 100947, https://doi.org/10.1016/j.jbc.2021.100947.

[35] J. Abramson, J. Adler, J. Dunger, R. Evans, T. Green, A. Pritzel, O. Ronneberger, L. Willmore, A.J. Ballard, J. Bambrick, S.W. Bodenstein, D.A. Evans, C.C. Hung, M. O'Neill, D. Reiman, K. Tunyasuvunakool, Z. Wu, A. Zemgulyte, E. Arvaniti, C. Beattie, O. Bertolli, A. Bridgland, A. Cherepanov, M. Congreve, A.I. Cowen-Rivers, A. Cowie, M. Figurnov, F.B. Fuchs, H. Gladman, R. Jain, Y.A. Khan, C.M. R. Low, K. Perlin, A. Potapenko, P. Savy, S. Singh, A. Stecula, A. Thillaisundaram, C. Tong, S. Yakneen, E.D. Zhong, M. Zielinski, A. Zidek, V. Bapst, P. Kohli, M. Jaderberg, D. Hassabis, J.M. Jumper, Accurate structure prediction of biomolecular interactions with AlphaFold 3, Nature 630 (2024) 493–500, https://doi.org/10.1038/s41586-024-07487-w.